

# Syntheses, Molecular Structures, and Bonding of Molybdenum and Tungsten Calix[4]arene Imido Complexes

Udo Radius\*<sup>[a]</sup> Juri Attner<sup>[a]</sup>

*Dedicated to Professor Dr. H. Werner on the occasion of his 65th birthday*

**Keywords:** Calixarenes / Inclusion compounds / Imido Complexes / Molybdenum / Tungsten

Syntheses, spectroscopic properties, molecular structures, and bonding of novel calix[4]arene imido compounds are described. Treatment of  $M(\text{N}t\text{Bu})_2(\text{NH}t\text{Bu})_2$  **1a** ( $M = \text{Mo}$ ), **1b** ( $M = \text{W}$ ) or  $M(\text{NMes})_2\text{Cl}_2(\text{dme})$  **2a** ( $M = \text{Mo}$ ), **2b** ( $M = \text{W}$ ) ( $\text{Mes} = 2,4,6\text{-Me}_3\text{-C}_6\text{H}_2$ ) with *p*-*t*Bu-calix[4]arene  $\text{LH}_4$  affords calix[4]arene metal complexes  $\text{LM}(\text{NR})$  **1a**, **b** ( $M = \text{Mo}, \text{W}$ ;  $R = t\text{Bu}$ ) and **2a**, **b** ( $M = \text{Mo}, \text{W}$ ;  $R = \text{Mes}$ ). Analytical and spectroscopic data are consistent with monomeric structures for **1** and **2**, retaining a local  $C_{4v}$  symmetry for the calix[4]arene metal fragment. These complexes are well-suited to bind small molecules like acetonitrile, *t*Bu-isonitrile, or water within their macrocyclic pockets. The spectroscopic data of some inclusion compounds and the crystal structures of  $\text{LMo}(\text{N}t\text{Bu})(\text{NCMe})$  **1a(NCMe)**,  $\text{LW}(\text{N}t\text{Bu})(\text{OH}_2)$  **1b(OH<sub>2</sub>)**,  $\text{LW}(\text{N}t\text{Bu})(\text{CN}t\text{Bu})$  **1b(CN*t*Bu)**,  $\text{LMo}(\text{NMes})(\text{NCMe})$  **2a(NCMe)**,

and  $\text{LW}(\text{NMes})(\text{NCMe})$  **2b(NCMe)** are reported. All complexes contain a group VI metal imido  $[\text{M}=\text{NR}]$  moiety mounted on the phenoxide rim of the calix[4]arene ligand as well as an incorporated guest molecule within the cavity. Some insights into the structures of complexes of the type  $\text{L}'\text{W}(\text{NR}')$  ( $\text{L}' = p\text{-H-calix[4]arene}$ ;  $\text{R}' = \text{H}, \text{Me}$ ) and into bonding in these compounds are provided by density functional theory, applying the B-P86 density functional and an all SVP basis set within the RI-J-DFT approximation. At least one  $\pi$  bond is of importance for calix[4]arene-metal bonding in these compounds. The metal-imido bond can be described as a triple bond. A geometrically optimized minimum structure of  $\text{L}'\text{W}(\text{NMe})$  **4** shows a calix[4]arene ligand only slightly distorted from a local  $C_{4v}$  symmetry and an almost linear tungsten-imido moiety.

## Introduction

The role of transition metal imido complexes<sup>[1]</sup> as reactive intermediates in industrial and laboratory organic synthesis<sup>[2][3]</sup> has received increased attention in recent years. The selective ammoxidation of propylene to acrylonitrile over bismuth molybdate catalysts with a minimal composition  $\text{Bi}_2\text{O}_3 \cdot n \text{MoO}_3$  is one of the most significant reactions of this type.<sup>[4]</sup> With approximately four million tons of worldwide acrylonitrile production, this process constitutes the largest volume example of an allylic oxidation process in industrial practice. Similar reactions employing methylbenzenes are used in the manufacture of benzonitriles and terephthalonitriles. It is known that in the ammoxidation ammonia is activated by the formation of a bismuth oxide supported imido species  $[\text{Mo}=\text{NH}]$ , and so this system has been the subject of industrial research and mechanistic studies.<sup>[5]</sup>

One approach leading to model oxo surfaces that bind metals on a molecular level is to employ ligands with a pre-organized set of oxygen donor atoms in a quasiplanar arrangement as provided, for example, by calixarenes.<sup>[6]</sup> The simplest of the calixarenes, the calix[4]arene system, usually binds in tetradentate fashion to transition metals and often retains its cone-like appearance.<sup>[7]</sup> As part of our ongoing

studies on metal-metal and metal-element multiple bonding supported by calix[4]arene ligands and calix[4]arene metal fragments,<sup>[8]</sup> we report here on the syntheses, molecular structures, and bonding of new molybdenum and tungsten calix[4]arene imido complexes.

## Results and Discussion

### Synthesis

There are, in principle, several ways to prepare *p*-*t*Bu-calix[4]arene organoimido complexes. Basic strategies are (i) to introduce the imido fragment into *p*-*t*Bu-calix[4]arene complexes and (ii) to introduce the *p*-*t*Bu-calix[4]arene fragment into imido complexes. Preparative ways for the former approach could be the reaction of *p*-*t*Bu-calix[4]arene metal chlorides  $\text{LMCl}_2$  with amines  $\text{RNH}_2$  in the presence of a base or the reaction of *p*-*t*Bu-calix[4]arene metal oxides  $\text{LM}=\text{O}$  with isocyanates  $\text{RN}=\text{C}=\text{O}$ .<sup>[1]</sup> Introduction of the *p*-*t*Bu-calix[4]arene fragment into imido complexes might be achieved by reacting imidochlorides  $\text{M}(\text{NR})\text{Cl}_4$  with *p*-*t*Bu-calix[4]arene  $\text{LH}_4$ . We decided to follow a similar method to that described by Gibson and co-workers for the preparation of a calix[4]arene imido molybdenum complex with the parent *p*-H-calix[4]arene. These authors reported the reaction of  $\text{M}(\text{NR})_2(\text{OtBu})_2$  with *p*-H-calix[4]arene  $\text{L}'\text{H}_4$ .<sup>[9]</sup> In the case of  $M = \text{Mo}$  and  $R = 2,6(i\text{Pr})_2\text{Ph}$  (Dip),<sup>[9a]</sup> formation of the calix[4]arene imido complex

<sup>[a]</sup> Institut für Anorganische Chemie, Engesserstr., Geb. 30.45, D-76128 Karlsruhe, Germany  
Fax: (internat.) + 49-721/661921  
E-mail: uradius@achibm6.chemie.uni-karlsruhe.de

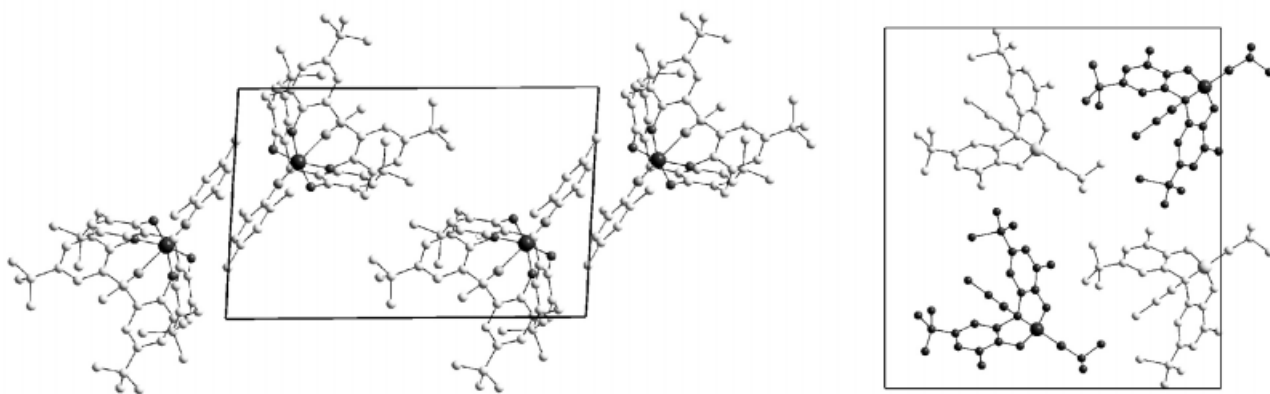


Figure 1. Packing diagram of  $\text{LMo}(\text{NMes})(\text{NCMe})$  **2a(NCMe)** (left side) and  $\text{LMo}(\text{N}t\text{Bu})(\text{NCMe})$  **1a(NCMe)** (right side). Projections down the  $a$  axis are shown. Molecules with the metal atom at  $(0.5, y, z)$  are light gray colored while those with metal atoms at  $(0, y, z)$  are dark gray colored in the cellplot of **1a(NCMe)**.

$\text{L}'\text{Mo}(\text{NDip})$  was observed, whereas in the case of  $\text{M} = \text{Cr}$  and  $\text{R} = t\text{Bu}$  all imido and alkoxy ligands were sacrificed to yield a mononuclear complex with two calix[4]arene molecules in the coordination sphere of the central chromium atom.<sup>[9b]</sup>

The  $p$ - $t\text{Bu}$ -calix[4]arene  $t\text{Bu}$ -imido complexes  $\text{LM}(\text{N}t\text{Bu})$  **1a** ( $\text{M} = \text{Mo}$ ) and **1b** ( $\text{M} = \text{W}$ ) are prepared by amide and imido replacement from compounds  $\text{M}(\text{N}t\text{Bu})_2(\text{NH}t\text{Bu})_2$ , which is a convenient starting material, especially for tungsten imido chemistry. Treatment of  $\text{M}(\text{N}t\text{Bu})_2(\text{NH}t\text{Bu})_2$  **1a** ( $\text{M} = \text{Mo}$ )<sup>[10a,10b]</sup> and **1b** ( $\text{M} = \text{W}$ )<sup>[10c,10d]</sup> with one equivalent of  $p$ - $t\text{Bu}$ -calix[4]arene  $\text{LH}_4$  in toluene affords the monoimido complexes  $\text{LMo}(\text{N}t\text{Bu})$  **1a** and  $\text{LW}(\text{N}t\text{Bu})$  **1b**, after work up, as high melting solids in moderate to good yield (see Scheme 1).

Since preliminary studies on the reactivity of **1a**, **b** revealed that these compounds do not readily decompose with traces of  $\text{HCl}$ ,<sup>[11]</sup> we tried to access calix[4]arene imido complexes by chloride and imido replacement from molybdenum and tungsten diimido dichlorides. These starting materials are also readily prepared and, especially for the molybdenum chemistry, more straightforward to synthesize than the amido imide **1a**. Treatment of  $\text{M}(\text{NMes})_2\text{Cl}_2(\text{dme})$  **IIa** ( $\text{M} = \text{Mo}$ ) and **IIb** ( $\text{M} = \text{W}$ ) ( $\text{Mes} = 2,4,6\text{-Me}_3\text{-C}_6\text{H}_2$ )<sup>[12]</sup> with one equivalent of  $p$ - $t\text{Bu}$ -calix[4]arene  $\text{LH}_4$  in refluxing toluene results in the formation of calix[4]arene

imido complexes  $\text{LMo}(\text{NMes})$  (**2a**) and  $\text{LW}(\text{NMes})$  (**2b**) in good yield. We believe this route to be general for the synthesis of compounds of the type  $\text{LM}(\text{NR})$  ( $\text{M} = \text{Mo}, \text{W}$ ).

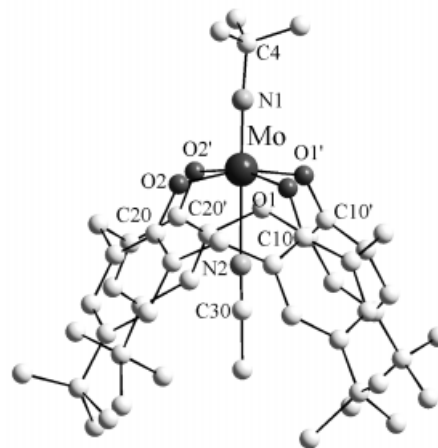
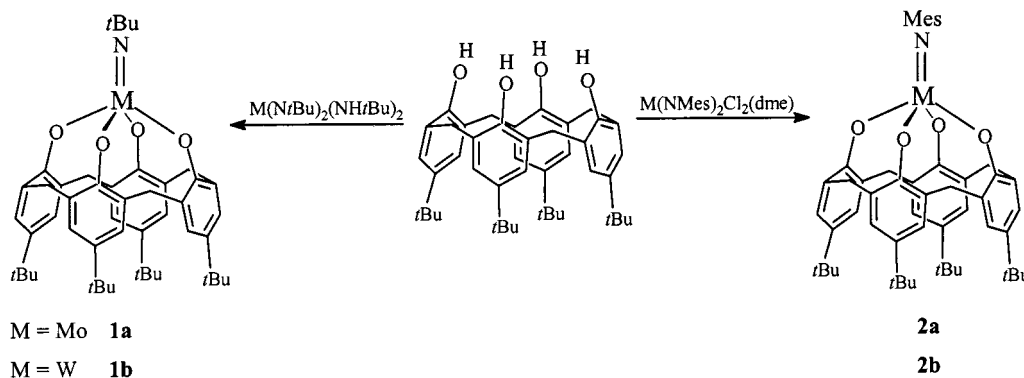


Figure 2. The molecular structure of  $\text{LMo}(\text{N}t\text{Bu})(\text{NCMe})$  **1a(NCMe)** with hydrogen atoms omitted for clarity. Disorders in  $t\text{Bu}$  groups are not resolved in the drawing. Selected bond lengths [pm] and angles [ $^\circ$ ]:  $\text{Mo}-\text{N1}$ : 171.8(10),  $\text{Mo}-\text{O1}$ : 194.0(5),  $\text{Mo}-\text{O2}$ : 194.0(5),  $\text{Mo}-\text{N2}$ : 234.3(9),  $\text{N1}-\text{C4}$ : 139.7(17),  $\text{O1}-\text{C10}$ : 134.0(9),  $\text{O2}-\text{C20}$ : 137.5(9),  $\text{C4}-\text{N1}-\text{Mo}$ : 176.9(11),  $\text{N1}-\text{Mo}-\text{O1}$ : 97.4(3),  $\text{N1}-\text{Mo}-\text{O2}$ : 97.6(3),  $\text{O1}-\text{Mo}-\text{O2}'$ : 165.0(2),  $\text{O2}-\text{Mo}-\text{O1}'$ : 165.0(2),  $\text{N1}-\text{Mo}-\text{N2}$ : 179.4(4),  $\text{C10}-\text{O1}-\text{Mo}$ : 129.6(5),  $\text{C20}-\text{O2}-\text{Mo}$ : 128.6(4).



Scheme 1

Unlike the calix[4]arene molybdenum oxide  $\text{LMo}=\text{O}$ ,<sup>[13]</sup> which coordinates an additional molecule  $\text{LH}_4$  to the  $\text{LMoO}$  core and is almost insoluble in common organic solvents, the imido compounds are readily soluble in organic solvents like benzene or toluene and sparingly soluble in hexane. The nature of the products was determined by  $^1\text{H}$ - and  $^{13}\text{C}$ -NMR spectroscopy as well as IR spectroscopy, mass spectroscopy, and elemental analysis. Analytical and spectroscopic data are consistent with a monomeric structure for **1** and **2** in the solid state and in solution. In all cases, intense signals for the molecular peaks were observed in the electron impact mass spectra at  $m/z = 813$  (**1a**), 899 (**1b**), 875 (**2a**), and 961 (**2b**).

The monomeric nature of these compounds in solution is also evident from NMR spectroscopy. The proton NMR spectra are typical for calix[4]arene complexes with a pseudo  $C_{4v}$  symmetry of the macrocyclic ligand, showing a singlet for the calix[4]arene *tert*-butyl protons, two doublets for the diastereotopic protons of the methylene bridges with a coupling constant between 12.1 and 12.5 Hz, and one resonance for the aromatic protons of the aryloxy groups.  $^1\text{H}$ -NOE measurements reveal that the doublet at lower field, for example at  $\delta = 4.47$  for the tungsten compound **1b**, is due to methylene hydrogen atoms closer to the metal atom, whereas the resonances at higher field, e.g. at  $\delta = 3.25$  for **1b**, have to be attributed to methylene protons in close proximity to the aryl hydrogen atoms. The proton NMR spectrum of a possible dinuclear imido-bridged species of the type  $\text{LM}(\mu\text{-NR})_2\text{ML}$ , in solution, should reveal the typical features of a calix[4]arene complex with local  $C_{2v}$  symmetry, i.e. a splitting of the signals of the *t*Bu protons of the inequivalent phenoxide rings. The local  $C_{4v}$  symmetry of the [LM] group is also reflected in the  $^{13}\text{C}\{^1\text{H}\}$ -NMR spectra of **1** and **2**, where we observed two signals for the calix[4]arene *tert*-butyl carbon atoms, one signal for the methylene bridges and four signals for the carbon atoms of the phenoxide ring.

Calixarenes have attracted some attention for their ability to include small guest molecules in the solid state.<sup>[6][14]</sup> In the X-ray structure determination of *p-t*Bu-calix[4]arene  $\text{LH}_4$ , for example, there was a toluene molecule incorporated into the *endo* calix position.<sup>[15]</sup> Despite considerable effort, we were unable to obtain good quality crystals of compound **1** or **2** without any guest molecule in the *endo* calix position or with toluene included into the calixarene basket. However, this situation changes when we allow **1** or **2** to react with small donor molecules like water, acetonitrile, or isonitrile.

Accordingly, the complexes  $\text{LMo}(\text{N}t\text{Bu})(\text{NCMe})$  **1a(NCMe)**,  $\text{LMo}(\text{N}t\text{Bu})(\text{CN}t\text{Bu})$  **1a(CNtBu)**,  $\text{LW}(\text{N}t\text{Bu})(\text{NCMe})$  **1b(NCMe)**,  $\text{LW}(\text{N}t\text{Bu})(\text{CN}t\text{Bu})$  **1b(CNtBu)**,  $\text{LW}(\text{N}t\text{Bu})(\text{OH}_2)$  **1b(OH<sub>2</sub>)**,  $\text{LMo}(\text{NMes})(\text{NCMe})$  **2a(NCMe)**, and  $\text{LW}(\text{NMes})(\text{NCMe})$  **2b(NCMe)** can be prepared by dissolving **1** or **2** in acetonitrile or by reaction of toluene solutions of **1** or **2** with nucleophiles like water, acetonitrile or isonitrile.

The IR spectra of the acetonitrile complexes show two bands in the characteristic region between 1700 and 2800

$\text{cm}^{-1}$ , one at approximately  $2320\text{ cm}^{-1}$ , the other at approximately  $2295\text{ cm}^{-1}$ . These bands may be assigned to a  $\text{C}\equiv\text{N}$  stretching frequency and a combination band, which results from coupling of a symmetric  $\text{CH}_3$  deformation mode and a  $\text{C}-\text{C}$  stretching frequency. The  $^1\text{H}$ -NMR spectra reveal one additional signal in the region of  $\delta = -0.1$  to  $-0.2$ , shifted upfield from the resonance of uncoordinated acetonitrile dissolved in  $\text{CDCl}_3$  at  $\delta = 1.90$ . Although coordination to transition metals might lead to upfield shifting of the acetonitrile resonances, these shifts are most probably due to shielding effects inside the cavity of the calix[4]arene ligand.

Similar shifts can be obtained for the isonitrile ligated to **1a** and **1b**. The resonances for the isonitrile  $\text{CH}_3$  groups at  $\delta = -0.17$  and  $-0.20$  are shifted significantly compared to the resonance of the uncoordinated molecule at  $\delta = 1.37$ . Bands at  $2211$  and  $2218\text{ cm}^{-1}$ , respectively, in the IR spectra of **1a(CNtBu)** and **1b(CNtBu)** are in the characteristic region of  $\text{C}\equiv\text{N}$  stretches. The bound  $\text{H}_2\text{O}$  molecule of **1b(OH<sub>2</sub>)** gives rise to two OH stretches at  $3519$  and  $3448\text{ cm}^{-1}$  in the IR spectrum, and a singlet at  $\delta = 1.54$  in the proton NMR spectrum.

$^{13}\text{C}$ -NMR spectroscopy has an exceptional position in the characterization of *tert*-butyl imido compounds.<sup>[1]</sup> The difference in the chemical shifts of  $\alpha$ - and  $\beta$ -*t*Bu-carbon atoms,  $\Delta\delta$ , can serve as an experimental probe for the electron density on the metal atom of imido complexes. A decrease of electron density on the metal atom leads to a strengthening of the metal-nitrogen bond and therefore to a decrease of electron density on the imido nitrogen atom. This decrease can be experimentally observed as a downfield shift of the  $\alpha$ -carbon atom resonance and a small upfield shift of the  $\beta$ -carbon atom resonance, and therefore by an increase of  $\Delta\delta$ . We observe a  $\Delta\delta$  value for  $\text{LW}(\text{N}t\text{Bu})$  **1b** of  $44.61\text{ ppm}$  and lower values for the adducts:  $40.47\text{ ppm}$  for **1b(NCMe)**,  $41.07\text{ ppm}$  for **1b(OH<sub>2</sub>)**, and  $41.36\text{ ppm}$  for **1b(CNtBu)**. Electron density on the metal atom increases upon coordination of the guest molecule and weakens the tungsten nitrogen bond of the calix[4]arene imido compound. This weakening is mainly due to  $\sigma$  bond effects (vide infra).

## Molecular Structures

Single crystal X-ray diffraction studies confirm the structural assignments for the calix[4]arene imido compounds of the type  $\text{LM}(\text{NR})$  deduced from spectroscopic data. Suitable crystals for X-ray analyses of the compounds  $\text{LMo}(\text{N}t\text{Bu})(\text{NCMe})$  **1a(NCMe)**,  $\text{LW}(\text{N}t\text{Bu})(\text{OH}_2)$  **1b(OH<sub>2</sub>)**,  $\text{LW}(\text{N}t\text{Bu})(\text{CN}t\text{Bu})$  **1b(CNtBu)**,  $\text{LMo}(\text{NMes})(\text{NCMe})$  **2a(NCMe)**, and  $\text{LW}(\text{NMes})(\text{NCMe})$  **2b(NCMe)** can either be grown from acetonitrile solutions (acetonitrile adducts) or toluene solutions (water adduct, isonitrile adduct). Projections of the cells down the *a* axis of  $\text{LMo}(\text{N}t\text{Bu})(\text{NCMe})$  **1a(NCMe)** and  $\text{LMo}(\text{NMes})(\text{NCMe})$  **2a(NCMe)** are given in Figure 1. The molecular structures of the compounds are shown in Figures 2 to 6, while selected bond lengths and

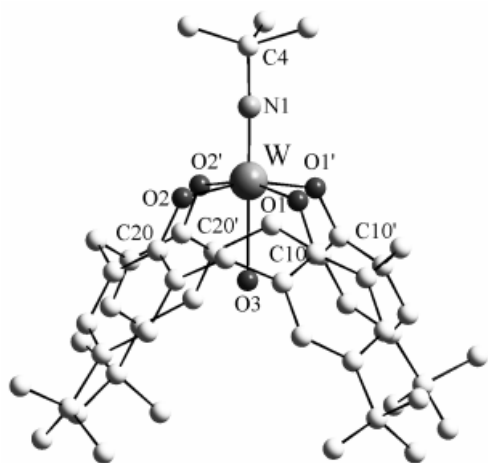


Figure 3. The molecular structure of  $\text{LW}(\text{NtBu})(\text{OH}_2)$  **1b(OH<sub>2</sub>)** with hydrogen atoms omitted for clarity. Disorders in *t*Bu groups are not resolved in the drawing. Selected bond lengths [pm] and angles [°]: W–N1: 171.8(5), W–O1: 194.4(3), W–O2: 193.6(3), W–O3: 230.3(4), N1–C4: 145.3(10), O1–C10: 136.4(5), O2–C20: 137.2(5), C4–N1–W: 171.7(7), N1–W–O1: 98.15(16), N1–W–O2: 98.33(16), O1–W–O2': 163.52(11), O2–W–O1': 163.52(11), N1–W–O3: 179.9, C10–O1–W: 129.5(2), C20–O2–W: 129.7(3).

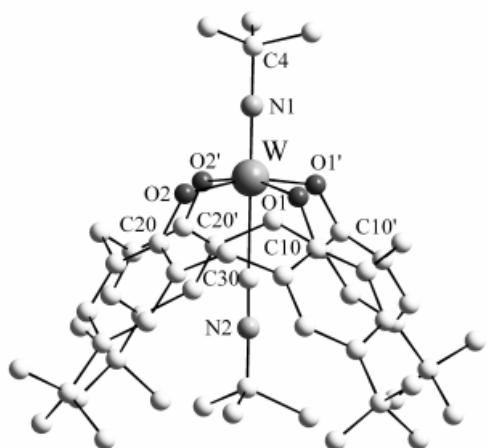


Figure 4. The molecular structure of  $\text{LW}(\text{NtBu})(\text{CNtBu})$  **1b(CNtBu)** with hydrogen atoms omitted for clarity. Disorders in *t*Bu groups are not resolved in the drawing. Selected bond lengths [pm] and angles [°]: W–N1: 173.0(10), W–O1: 192.5(6), W–O2: 193.7(6), W–O3: 241.7(13), N1–C4: 145(2), O1–C10: 138.7(12), O2–C20: 136.4(11), C30–N2: 118.9(18), C4–N1–W: 177.6(17), N1–W–O1: 97.8(3), N1–W–O2: 98.5(3), N1–W–O3: 179.8(5), O1–W–O2': 163.7(2), O2–W–O1': 163.7(2), N2–C30–W: 179.0(10), C10–O1–W: 130.6(5), C20–O2–W: 130.3(6).

bond angles are given in the figure captions. Some important structural parameters are summarized and compared in Table 1.

Compound **2a(NCMe)** crystallizes in the triclinic space group  $P\bar{1}$ , **2b(NCMe)** in  $Cc$ , and the isostructural *tert*-butyl imido compounds **1a(NCMe)**, **1b(OH<sub>2</sub>)**, and **1b(CNtBu)** in the orthorhombic space group  $Cmc2_1$ . As shown on the left side of Figure 1, the molecules of the molybdenum mesityl imido compound **2a(NCMe)** are in a head-to-head arrangement connected through  $\pi$  stacking of the aryl rings of the imido ligand. The carbon-carbon distances of the mutually

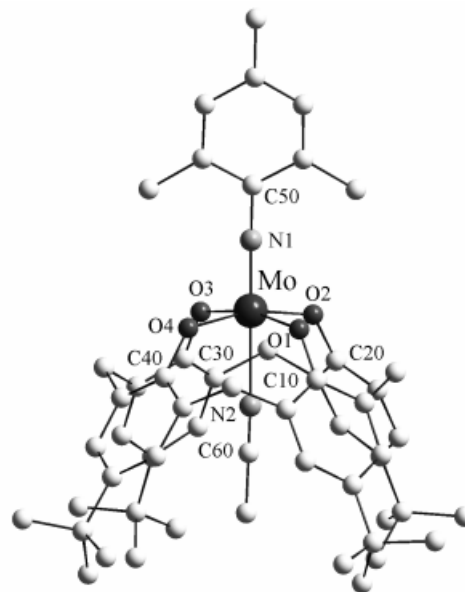


Figure 5. The molecular structure of  $\text{LMo}(\text{NMes})(\text{NCMe})$  **2a(NCMe)** with hydrogen atoms omitted for clarity. Disorders in *t*Bu groups are not resolved in the drawing. Selected bond lengths [pm] and angles [°]: Mo–N1: 172.4(3), Mo–O1: 194.8(3), Mo–O2: 193.7(2), Mo–O3: 193.9(3), Mo–O4: 195.3(2), Mo–N2: 230.3(3), N1–C50: 137.9(3), N2–C60: 113.3(4), O1–C10: 136.0(3), O2–C20: 137.1(4), O3–C30: 136.8(3), O4–C40: 136.3(3), Mo–N1–C50: 172.3(2), Mo–N2–C60: 177.8(4), N1–Mo–O1: 95.87(11), N1–Mo–O2: 98.07(11), N1–Mo–O3: 98.11(11), N1–Mo–O4: 97.04(11), O1–Mo–O3: 165.92(8), O2–Mo–O4: 164.85(8), N1–Mo–N2: 177.56(10), C10–O1–Mo: 128.99(17), C20–O2–Mo: 128.4(3), C30–O3–Mo: 125.80(16), C40–O4–Mo: 131.38(17).

opposite atoms are in a narrow range between 371.7–372.5 pm. The other structurally characterized compounds are close to isostructural and show molecules isolated from each other in the unit cell, as presented for **1a(NCMe)** at the right side of Figure 1.

All complexes contain a group VI metal imido  $\text{M}=\text{NR}$  moiety mounted on the phenoxide rim of the calix[4]arene ligand. The four oxygen atoms of the calix[4]arene ligand and the nitrogen atom of the imido ligand span a flat square pyramidal environment around the transition metal atom. A sixth coordination site is occupied by a neutral donor molecule, i.e. acetonitrile, isonitrile, or water, respectively. Thus, the metal atoms adopt distorted octahedral coordination spheres.

The donor atoms of the guest molecules are almost linearly coordinated to the metal atoms with respect to the metal–(imido)nitrogen vector and all N1–M–D angles are larger than 177°. The distances and angles of the coordinated acetonitrile molecules suggest minimal changes in the bonding of these ligands compared to the uncomplexed molecules, because the  $d^0$  metal centers cannot  $\pi$  backdonate into the carbon-nitrogen triple bonds. The carbon–nitrogen distances of 111.4(15) pm in **1a(NCMe)**, 113.3(4) pm in **2a(NCMe)**, and 112.0(6) pm in **2b(NCMe)**, as well as almost linear [N–C–C] entities, indicate carbon-nitrogen bond orders of approximately three. The bond lengths of the acetonitrile adducts compare well with other aceto-



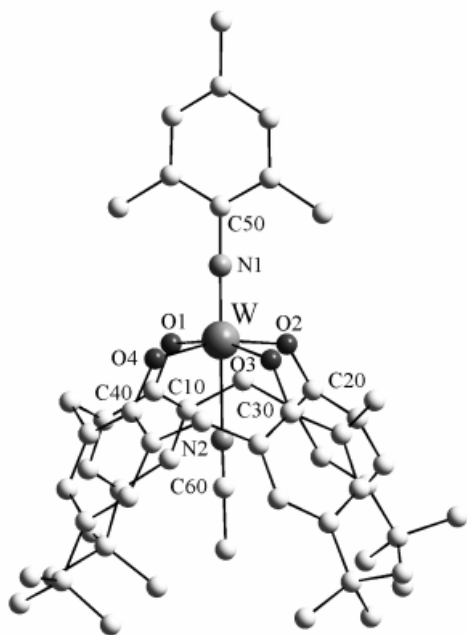


Figure 6. The molecular structure of LW(NMes)(NCMe) **2b(NCMe)** with hydrogen atoms omitted for clarity. Selected bond lengths [pm] and angles [°]: W–N1: 174.3(4), W–O1: 194.0(3), W–O2: 194.0(3), W–O3: 194.5(3), W–O4: 194.6(3), W–N2: 231.4(3), N1–C50: 138.0(5), N2–C60: 112.0(6), O1–C10: 136.9(5), O2–C20: 135.6(5), O3–C30: 136.6(5), O4–C40: 137.4(5), C50–N1–W: 177.5(3), C60–N2–W: 178.5(3), N1–W–O1: 98.16(14), N1–W–O2: 97.41(15), N1–W–O3: 97.78(16), N1–W–O4: 97.99(15), O1–W–O3: 164.06(12), O2–W–O4: 164.60(12), N1–W–N2: 179.44(14), C10–O1–W: 129.5(3), C20–O2–W: 131.0(2), C30–O3–W: 129.6(2), C40–O4–W: 128.7(2).

Table 1. Comparison of selected bond lengths [pm] and angles [°] of LMo(NrBu)(NCMe) **1a(NCMe)**, LW(NrBu)(OH<sub>2</sub>) **1b(OH<sub>2</sub>)**, LW(NrBu)(CNrBu) **1b(CNrBu)**, LMo(NMes)(NCMe) **2a(NCMe)**, and LW(NMes)(NCMe) **2b(NCMe)**

	<b>1a(NCMe)</b>	<b>1b(OH<sub>2</sub>)</b>	<b>1b(CNrBu)</b>	<b>2a(NCMe)</b>	<b>2b(NCMe)</b>
M–N	171.8	171.8	173.0	172.4	174.3
M–O	194.0 194.0	194.4 193.6	192.5 193.7	193.7 193.9 194.8 195.3	194.0 194.0 194.5 194.6
M–D	234.3	230.3	241.7	230.3	231.4
N2–C	111.4		118.9	113.3	112.0
M–N1–C	176.9	171.7	177.6	172.3	177.5
N1–M–O	97.4 97.6	98.2 98.3	97.8 98.5	95.9 97.0 98.1 98.1	97.4 97.8 98.0 98.2
N1–M–D	179.4	179.9	179.8	177.6	179.4
M–O–C	129.6 128.6	129.5 129.7	130.6 130.3	125.8 128.4 129.0 131.5	128.7 129.5 131.0
(O–M–O) <sub>trans</sub>	165.0	163.5	163.7	165.9 164.9	164.1 164.6

nitrile adducts of group VI imido complexes of metals in their highest oxidation state.<sup>[16]</sup> The N–C bond lengths of the acetonitrile molecules in **2a(NCMe)**, **2b(NCMe)**, and **1a(NCMe)** correlate with the lengths of the M–N2 bonds of 230.3(3) pm in **2a(NCMe)**, 231.4(3) pm in **2b(NCMe)**, and 234.4(9) pm in **1a(NCMe)**.

Compound **1b(CNrBu)** is the first structurally characterized terminal isonitrile complex of a d<sup>0</sup>-group VI metal complex. The observed W–C bond length in **1b(CNrBu)** of 241.7(13) pm is very long compared to homoleptic W<sup>II</sup> complexes [W(CNrBu)<sub>7</sub>]<sup>2+</sup>. In these compounds, W–C distances are in a range between 206.9(6) pm and 214.2(8) pm.<sup>[17]</sup> The W–OH<sub>2</sub> bond length of 230.3(4) pm in **1b(OH<sub>2</sub>)** is significantly shorter than the Mo–OH<sub>2</sub> distance of 240.8(16) pm in the calix[4]arene molybdenum oxide (LH<sub>4</sub>)LMoO(OH<sub>2</sub>)(PhNO<sub>2</sub>),<sup>[13]</sup> but comparable to other tungsten complexes with a water molecule coordinated *trans* to σ,π donor ligands. In tungsten(V) anions of the type [W(=O)X<sub>4</sub>(OH<sub>2</sub>)]<sup>−</sup> prepared by Atwood and co-workers, for example, the W–OH<sub>2</sub> bond length comes to 226.2(9) pm (X = Cl) and 231(2) pm (X = Br), respectively, and in an anion of higher nuclearity prepared in Jeannin's group the W–OH<sub>2</sub> bond length was determined to be 229(1) pm.<sup>[18]</sup>

The calix[4]arene metal fragments of all the imido compounds LM(NR)(donor) that were investigated by X-ray crystallography retain pseudo C<sub>4v</sub> symmetry in the solid state and produce circular calix[4]arene cavities similar to those in the uncoordinated ligand. The molybdenum–oxygen and tungsten–oxygen bond lengths are in a very narrow range between 192.5(6) pm and 195.3(2) pm, with three exceptions at 194.0±0.6 pm, and are comparable with average metal–oxygen bond lengths in molybdenum or tungsten aryloxy complexes.<sup>[19]</sup> The angles N1–M–O are between 97° and 99°, the angles M–O–C are approximately 130° and all *endo* calix angles O–M–O between two *trans* oxygen atoms are in a narrow range between 163.5° and 165.9°.

The short Mo–N1 and W–N1 contacts of 171.8(5)–174.3(4) pm and the almost linear M–N1–C entities with angles larger than 170° suggest sp hybridized imido nitrogen atoms with triple bond character of the metal–(imido)-nitrogen bond.<sup>[1]</sup> These bonding parameters are also in good agreement with other monoimido complexes of the type Mo(NR)X<sub>4</sub>·L, for example in Mo(NTolyl)Cl<sub>4</sub>·THF [Mo–N bond length 171.7(3) pm, angle Mo–N–C 174.6(3)°],<sup>[20]</sup> in (H<sub>2</sub>NSO<sub>2</sub>N)WCl<sub>4</sub>·NCMe [W–N bond length 173.0(12) pm, angle W–N–S 168.3(7)°],<sup>[16b]</sup> in (ClN)WCl<sub>4</sub>·NCMe [W–N bond length 172(1) pm, angle W–N–C 175.5(10)°]<sup>[16c]</sup> or in L'Mo(NDip) [Mo–N bond length 172.9(3) pm, angle Mo–N–C 179.2(2)°].<sup>[9a]</sup>

## Theoretical Studies

In order to gain some insight into the bonding situation of calix[4]arene imido complexes, as well as their donor adducts, we performed density functional calculations<sup>[21]</sup> on

model compounds of the characterized complexes. We wanted to understand calix[4]arene–metal bonding, bonding of the imido fragment [RN] to the calix[4]arene metal fragment [LM] and the influence of the donor molecule on metal–imido bonding. The *t*Bu groups of the calix[4]arene ligands were replaced by hydrogen atoms and the organic groups of the imido ligands were replaced by hydrogen or methyl groups to reduce computational cost. The models under investigation were the tungsten compounds L'W(NH) **3** and L'W(NMe) **4** (L' = *p*-H-calix[4]arene).

For an electron count of calix[4]arene imido complexes, we opted to cleave all metal ligand bonds heterolytically and end up with [L']<sup>4−</sup>, a metal center in the formal electron configuration d<sup>0</sup> and a closed shell imido anion [NR]<sup>2−</sup>. Counting the imido ligand – in agreement with the M–N bond lengths (vide supra) – as a six-electron donor,<sup>[1]</sup> the calix[4]arene ligand has to provide 12 electrons for an 18 VE count on the central atom. For the acetonitrile- and isonitrile-stabilized complexes, 10 electrons are sufficient since these donor molecules act as neutral two electron donors. Eight electrons are provided by four σ bonds. Thus, one [for LM(NR)(D) type complexes] and two [for LM(NR) type complexes] calix[4]arene–metal π bonds are necessary to fulfill the 18 VE rule for the central atom. In the evaluation of π bonding in this type of compound, we want to preface our analysis with simple considerations emerging from group theory.

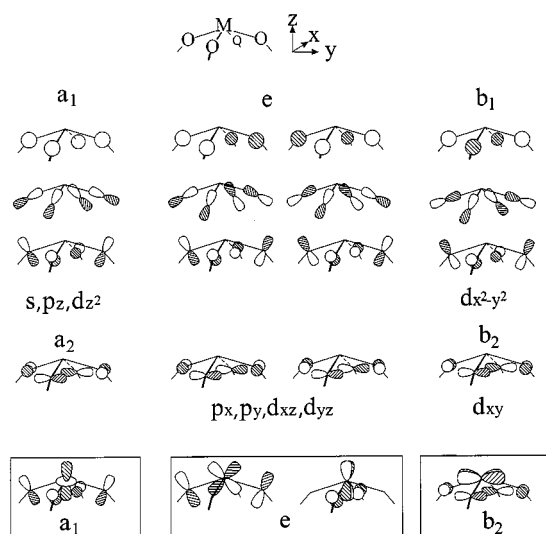


Figure 7. Symmetry-adapted linear combinations of oxygen s and p orbitals of a  $C_{4v}$  [O<sub>4</sub>] set

One possibility to generate symmetry adapted combinations of oxygen s and p orbitals of an [O<sub>4</sub>] fragment in  $C_{4v}$  symmetry is shown in Figure 7. Combination of the oxygen s orbitals gives four symmetry adapted orbitals that transform as a<sub>1</sub>, e, and b<sub>1</sub>, which are shown as the first entry in Figure 7. For the p orbitals on each oxygen atom, one can think of a basis set independent from the cartesian coordinate system, one radial p orbital pointing in the direction of the M–O vector and two sets of tangential p orbitals, which are perpendicular to each other and to the

M–O vector (second and third entry in Figure 7). The radial p orbitals and one of the tangential sets transform as a<sub>1</sub>, e, and b<sub>1</sub>. The second set of tangential orbitals, those lying in the O<sub>4</sub> plane, transforms as a<sub>2</sub>, e, and b<sub>2</sub> (fourth entry in Figure 7). The counterparts on the metal atom, which can interact with these combinations, are s, p<sub>z</sub>, and d<sub>z<sup>2</sup></sub> for a<sub>1</sub> ligand orbitals, p<sub>x</sub>, p<sub>y</sub>, d<sub>xz</sub>, and d<sub>yz</sub> for ligand orbitals of e symmetry, d<sub>x<sup>2</sup>−y<sup>2</sup></sub> for b<sub>1</sub>, and d<sub>xy</sub> for b<sub>2</sub> ligand orbitals. Within this simplified scheme, linear combinations of radial ligand p orbitals and ligand s orbitals are responsible for metal ligand σ bonding, whereas π bonding comes from overlap of tangential ligand orbitals with metal orbitals of appropriate symmetry. The most important interactions for π bonding are shown in the lowest part of Figure 7. There is one π interaction of a<sub>1</sub> symmetry, one of e symmetry and one of b<sub>2</sub> symmetry. For the  $C_{4v}$  calix[4]arene metal fragment we observe M–O–C angles of approximately 130°, a value that is significantly smaller than 180°. Thus, there will be mixing of radial and tangential orbitals of the same symmetry resulting in a good O–C overlap and, as a consequence of this, in worse overlap of the a<sub>1</sub> and e π-type orbitals shown at the bottom of Figure 7.

In order to check these qualitative considerations, DFT calculations were carried out on geometrically optimized  $C_{4v}$  L'W(NH) **3** and on the complex fragment  $C_{4v}$  [L'W]<sup>2+</sup>. The imido complex **3** optimizes at W–O distances of 195.8 pm, a W–N distance of 174.8 pm and angles W–O–C of 135.6°. These bonding parameters are in good agreement with the experimental results. The imido group is kept linear to retain overall  $C_{4v}$  symmetry. A Mulliken population analysis of the tungsten-oxygen bond reveals a strong π bond for the b<sub>2</sub> orbital shown at the bottom of Figure 7. The contribution of the irreducible representation b<sub>2</sub> is 0.106 to a total W–O overlap population of 0.420. In contrast, contributions from e-type orbitals are almost negligible. Similar results can be obtained from an SEN (shared electron number) analysis<sup>[22]</sup> of covalent contributions to the W–O bond. Orbitals of b<sub>2</sub>-type symmetry contribute significantly to the W–O bond (0.169 out of a total of 0.611), whereas the contributions of e symmetry are approximately 0.03. Calculations on the complex fragment [L'W]<sup>2+</sup> confirm these results. The b<sub>2</sub> interaction shown in the lowest part of Figure 7 is an important π interaction that helps to stabilize metal d orbitals in calix[4]arene metal complexes.

A truncated fragment molecular orbital (FMO) scheme for the interaction of a  $C_{4v}$  calix[4]arene tungsten fragment [L'W]<sup>2+</sup> with a linear dianionic imido group [NR]<sup>2−</sup> is shown in Figure 8. The frontier orbitals of the [L'W]<sup>2+</sup> complex fragment are shown schematically on the left side. A group of highest occupied orbitals indicated as a dashed box are centered on the calix[4]arene ligand, mainly on the carbon atoms of the phenoxide. The highest unoccupied orbitals are metal-centered and give a typical M(ligand)<sub>4</sub> pattern: there is a low lying 1a<sub>1</sub> orbital, mainly d<sub>z<sup>2</sup></sub> in character, a degenerate set of d<sub>xz</sub> and d<sub>yz</sub> orbitals of e symmetry, a W–O antibonding orbital of b<sub>2</sub> symmetry (d<sub>xy</sub>), and two orbitals 2a<sub>1</sub> (p<sub>z</sub>) and b<sub>1</sub> (d<sub>x<sup>2</sup>−y<sup>2</sup>) that are high in energy. Im-</sub>

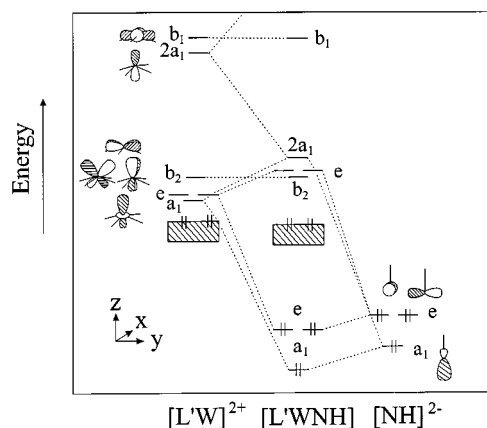


Figure 8. Schematic FMO diagram for  $C_{4v}$   $L'W\equiv NH$  built up from the components  $[L'W]^{2+}$  (left side) and  $[NR]^{2-}$  (right side). The important frontier orbitals of the fragments and the combined molecule are shown. The HOMO region of  $[L'W]^{2+}$  and  $L'W\equiv NH$  is indicated by a dashed box.

portant orbitals of the linear imido fragment  $[NR]^{2-}$  are an sp hybrid orbital of  $a_1$  symmetry and a degenerate e set of nitrogen  $p_x$  and  $p_y$  orbitals, and these are shown on the right side of Figure 8. The W–N  $\sigma$  bond is built up from interactions of the  $a_1$  orbitals depicted in Figure 8, with some additional admixture of tungsten s. The orbitals of e symmetry combine to give a degenerate set of  $\pi$  orbitals for the tungsten nitrogen bond. The net result of this interaction is a metal–nitrogen triple bond resulting from one  $\sigma$ –( $a_1$ ) and two  $\pi$ –(e) interactions. This qualitative picture is confirmed by our DFT results on  $C_{4v}$   $L'W(NH)$  **3**. From a total shared electron number (SEN) of 1.59 electrons for the tungsten nitrogen bond, 0.83 electrons are due to contributions of  $a_1$  symmetry and 0.76 electrons are due to contributions of e symmetry.

A detailed analysis of the frontier orbitals of  $C_{4v}$   $L'W(NH)$  **3** shows that HOMO 30e is a ligand centered orbital, whereas LUMO 13b<sub>2</sub> is tungsten  $d_{xy}$  in character. The LUMO + 1, a degenerate orbital 31e is W–N antibonding and can be considered a W–N  $\pi^*$  orbital. The LUMO + 2, which is also W–N antibonding, is an  $a_1$  hybrid orbital with contributions from tungsten  $d_{z^2}$ ,  $p_z$ , and s, as well as some nitrogen s and  $p_z$ . This orbital is responsible for binding an *endohedral* donor molecule, such as nitriles or isonitriles, to the metal atom. Calculations on **3(NCH)** show that the W–(imido)N bond should be weaker in comparison to **3**, mainly due to a lower  $a_1$  contribution to the W–(imido)N bond.

An X-ray crystal structure of  $L'Ta(\eta^5-C_5Me_5)$ ,<sup>[23]</sup> which is isoelectronic to  $L'W(NR)$ , shows a significant distortion from pseudo  $C_{4v}$  to pseudo  $C_{2v}$  symmetry for the macrocycle bound to the CpTa unit, and this results in an *elliptical* cone section for the calix[4]arene ligand. This distortion can be traced by two sets of different Ta–O bond lengths (189 pm and 200 pm), two sets of Ta–O–C angles (one set with angles larger than 160°, the other with angles of approximately 125°) and two different *endo* calix angles (127° and 155°). Lippard and co-workers attributed this distortion to favorable oxygen-to-metal  $\pi$  bonding for the distorted mol-

ecule. The opening of one pair of the M–O–C angles should lead to a better overlap for one of the  $\pi$  bonds of the e set depicted at the bottom of Figure 7. However, the optimization of  $L'W(NH)$  **3** under  $C_{2v}$  symmetry restriction leads to a geometry that is only 0.03 kcal/mol lower in energy than  $C_{4v}$   $L'W(NH)$ , and only minor deviations from the  $C_{4v}$  structure can be observed. The calculated bond lengths and angles in  $C_{2v}$   $L'W(NH)$  are 174.8 pm [in  $C_{4v}$   $L'W(NH)$ : 174.8 pm] for the W–N bond, 196.5 pm and 194.8 pm (195.8 pm) for the different W–O bonds, 104.0 and 102.6° (103.2°) for the angles N–W–O, and 131.9° and 140.0° (135.6°) for the W–O–C angles.

Since we were not able to obtain high quality crystals of compounds **1** and **2** without any guest in the calix[4]arene cavity, we decided to optimize an extended model system,  $L'WNMe$  **4**, without any symmetry restraints in order to answer the question as to whether the calix[4]arene ligand in these group VI imido compounds adopts pseudo  $C_{4v}$  symmetry or distorts to a pseudo  $C_{2v}$ -type structure with an *elliptical* cone section. The geometrically optimized minimum structure of  $L'W(NR')$  **4** shows the calix[4]arene ligand to be only slightly distorted from a local  $C_{4v}$  structure and an almost linear tungsten-imido moiety. We calculate a W–N distance of 174.91 pm and an angle W–N–C of 179.95°, W–O distances of 196.33±2 pm, W–O–C angles of 134.74±2°, and N–W–O angles of 102.62±2°. The bond lengths obtained are in good agreement with those of the experimentally determined structures (see Table 1), while the angles N–W–O and W–O–C are significantly smaller in the observed structures due to coordination of an additional molecule inside the calix[4]arene cavity. However, there is no driving force for a significant distortion in these systems as reported for the tantalum compound. The tungsten  $d_{xz}$  and  $d_{xy}$  orbitals of e symmetry are significantly stabilized by interaction with a good  $\sigma$ ,  $\pi$  donor, i.e. the imido ligand, and do not contribute to tungsten calix[4]arene bonding.

## Conclusions

Group VI calix[4]arene imido complexes  $LM(NR)$  **1a, b** ( $M = Mo, W$ ;  $R = tBu$ ) and **2a, b** ( $M = Mo, W$ ;  $R = Mes$ ) have been prepared and characterized. Treatment of  $M(NtBu)_2(NHtBu)_2$  or  $M(NMes)_2Cl_2(dme)$  ( $M = Mo, W$ ) with *p*-*t*Bu-calix[4]arene  $LH_4$  affords calix[4]arene metal imido complexes  $LM(NR)$  **1a, b** ( $M = Mo, W$ ;  $R = tBu$ ) and **2a, b** ( $M = Mo, W$ ;  $R = Mes$ ). These molecules are well suited to bind small molecules, like acetonitrile, *t*Bu-isonitrile, or water within their macrocyclic pockets, and some of those adducts have also been characterized. The monomeric nature of these compounds in solution is demonstrated by NMR spectroscopy. <sup>1</sup>H- and <sup>13</sup>C-NMR spectra are typical for calix[4]arene complexes with a pseudo  $C_{4v}$  symmetry of the macrocyclic ligand. The signals of the acetonitrile and isonitrile molecules incorporated into the *endo* calix site are shifted significantly in the <sup>1</sup>H-NMR spectra as compared to the uncoordinated guest molecules.



The crystal structures of  $\text{LMo}(\text{N}t\text{Bu})(\text{NCMe})$  **1a(NCMe)**,  $\text{LW}(\text{N}t\text{Bu})(\text{OH}_2)$  **1b(OH<sub>2</sub>)**,  $\text{LW}(\text{N}t\text{Bu})(\text{CN}t\text{Bu})$  **1b(CN $t$ Bu)**,  $\text{LMo}(\text{NMes})(\text{NCMe})$  **2a(NCMe)**, and  $\text{LW}(\text{NMes})(\text{NCMe})$  **2b(NCMe)** show a group VI metal imido  $\text{M}=\text{NR}$  moiety mounted on the phenoxide rim of the calix[4]arene ligand and an incorporated guest molecule within the cavity. The metal atoms in these compounds adopt a distorted octahedral coordination sphere. The calix[4]arene ligands also retain a pseudo  $C_{4v}$  symmetry in the solid state and thus produce circular calix[4]arene cavities. The imido group  $[\text{M}-\text{N}-\text{R}]$  is almost linear with  $\text{M}-\text{N}$  distances of 171.8(5)–174.3(4) pm. In the solid state, molecules of  $\text{LMo}(\text{NMes})(\text{NCMe})$  **2a(NCMe)** are assembled head-to-head through van der Waals forces between the aryl rings of the imido ligands.

Some insights into the structures of compounds of the type  $\text{L}'\text{W}(\text{NR}') \mathbf{3}$  and  $\mathbf{4}$  ( $\text{L}' = p\text{-H-calix[4]arene}$ ;  $\text{R}' = \text{H}$ , Me) and into bonding in calix[4]arene imido complexes are provided by density functional theory. Simple symmetry considerations show that there is one  $\pi$  bond of  $b_2$  symmetry, which is very important for calix[4]arene–metal bonding in these compounds. This is confirmed by population analyses of  $C_{4v}$   $\text{L}'\text{W}(\text{NH}) \mathbf{3}$ . The geometrically optimized minimum structure of  $\text{L}'\text{W}(\text{NR}') \mathbf{4}$  shows the calix[4]arene ligand only slightly distorted from a local  $C_{4v}$  structure and an almost linear tungsten-imido moiety. According to our DFT results, calix[4]arene–tungsten  $\pi$  interactions of  $e$  symmetry do not contribute significantly to the net stabilization of this compound.

## Experimental Section

**General:** All reactions and subsequent manipulations involving organometallic reagents were performed under an argon atmosphere using standard Schlenk techniques. The preparation of samples for spectroscopy was undertaken using a glove box (Braun MB 150 BG-I). Solvents were dried according to standard procedures, stored over activated 4-Å molecular sieves and degassed prior to use. Deuterated solvents were obtained from Aldrich Inc. (all 99 atom% D), dried according to standard procedures, and stored over activated 4-Å molecular sieves. – NMR spectra were recorded on a Bruker AC 250 at 298 K.  $^{13}\text{C}$ -NMR spectra are broad-band proton decoupled ( $^{13}\text{C}\{^1\text{H}\}$ ). Standard DEPT-135 experiments were recorded to distinguish  $-\text{CH}_3$ - and  $-\text{CH}$ -type carbons from  $-\text{C}-$  or  $-\text{CH}_2$ -type carbons in the  $^{13}\text{C}$ -NMR spectrum. NMR data are listed in parts per million (ppm) and are reported relative to tetramethylsilane. Coupling constants are quoted in Hertz. Residual solvent peaks used as internal standards were as follows:  $\text{CDCl}_3$ :  $\delta = 7.24$  ( $^1\text{H}$ ),  $\text{CD}_2\text{Cl}_2$ :  $\delta = 5.32$  ( $^1\text{H}$ ) or natural-abundance carbon signal at  $\delta = 77.0$  for  $\text{CDCl}_3$  and  $\delta = 54.0$  for  $\text{CD}_2\text{Cl}_2$ . – EI-MS spectra were recorded on a Varian MAT 3830 (70 eV). – Elemental analyses were performed by the microanalytical laboratory of the author's department. – Infrared spectra were recorded as KBr pellets on a Bruker IFS 28 and are reported in  $\text{cm}^{-1}$ . – The compounds  $p\text{-}t\text{Bu-calix[4]arene}$ ,<sup>[24]</sup>  $\text{Mo}(\text{NH}t\text{Bu})_2(\text{N}t\text{Bu})_2$ ,<sup>[10a,10b]</sup>  $\text{W}(\text{NH}t\text{Bu})_2(\text{N}t\text{Bu})_2$ ,<sup>[10c,10d]</sup> and  $[\text{M}(\text{NMes})_2\text{Cl}_2(\text{dme})]$  ( $\text{M} = \text{Mo}$ , W)<sup>[12]</sup> were prepared as described in the literature. All other reagents were purchased from commercial sources and purified by standard techniques.

**Preparation of  $p\text{-tert-Butylcalix[4]arene-tert-butylimidomolybdenum(VI)}$  (**1a**):** A solution of 250 mg (0.65 mmol) of  $\text{Mo}(\text{NH}t\text{Bu})_2(\text{N}t\text{Bu})_2$  and 485 mg (0.65 mmol) of  $p\text{-}t\text{Bu-calix[4]arene}$  toluene adduct in 40 mL of toluene was stirred for 8 h at 80°C. All volatile material was removed in vacuo. The red-brown residue was washed with 20 mL of hexane, collected, and dried in vacuo. Yield: 435 mg, 82%. m.p. 345°C (dec.). Crystals suitable for X-ray analysis were grown from a saturated acetonitrile solution of **1a** to yield **1a(NCMe)**. **1a(CN $t$ Bu)** was obtained as a red-brown powder by addition of an excess of  $t\text{Bu-isocyanide}$  to a toluene solution of **1a** and removal of all volatiles in vacuo. –  $^1\text{H}$  NMR ( $\text{CDCl}_3$ ) [**1a**]:  $\delta = 7.10$  (s, 8 H, aromatic  $H$ ), 4.36 (d, 4 H,  $^2J_{\text{HH}} = 12.3$  Hz,  $\text{CH}_2$ ), 3.24 (d, 4 H,  $^2J_{\text{HH}} = 12.3$  Hz,  $\text{CH}_2$ ), 1.85 [s, 9 H,  $\text{NC}(\text{CH}_3)_3$ ], 1.25 [s, 36 H,  $\text{C}(\text{CH}_3)_3$ ]. –  $^{13}\text{C}$  NMR ( $\text{CDCl}_3$ ) [**1a**]:  $\delta = 29.28$  [s,  $\text{NC}(\text{CH}_3)_3$ ], 31.49 [s,  $\text{C}(\text{CH}_3)_3$ ], 33.86 (s,  $\text{CH}_2$ ), 34.09 [s,  $\text{C}(\text{CH}_3)_3$ ], 81.99 [s,  $\text{NC}(\text{CH}_3)_3$ ], 124.96 (s, aromatic CH), 130.22 (s, aromatic C), 145.76 (s, aromatic  $\text{C}t\text{Bu}$ ), 153.96 (s, aromatic CO). – EI/MS (70 eV)  $m/z$  (%): 813 [ $\text{M}]^+$  (87), 798 [ $\text{M} - \text{CH}_3$ ] $^+$  (3), 756 [ $\text{M} - \text{C}_4\text{H}_9$ ] $^+$  (49), 741 [ $\text{M} - \text{NC}_4\text{H}_9$ ] $^+$  (21), 57 [ $\text{C}(\text{CH}_3)_3$ ] $^+$  (38), 41 [ $\text{C}_3\text{H}_5$ ] $^+$  (100). –  $\text{C}_{48}\text{H}_{61}\text{O}_4\text{MoN}$  (811.96) calcd. C 71.00, H 7.57, N 1.73; found C 70.91, H 7.63, N 1.71.

$^1\text{H}$  NMR ( $\text{CDCl}_3$ ) [**1a(NCMe)**]:  $\delta = 7.04$  (s, 8 H, aromatic  $H$ ), 4.32 (d, 4 H,  $^2J_{\text{HH}} = 12.1$  Hz,  $\text{CH}_2$ ), 3.14 (d, 4 H,  $^2J_{\text{HH}} = 12.2$  Hz,  $\text{CH}_2$ ), 1.86 [s, 9 H,  $\text{NC}(\text{CH}_3)_3$ ], 1.15 [s, 36 H,  $\text{C}(\text{CH}_3)_3$ ],  $-0.16$  (s, 3 H, MeCN). –  $^{13}\text{C}$  NMR ( $\text{CDCl}_3$ ) [**1a(NCMe)**]:  $\delta = 28.78$  [s,  $\text{NC}(\text{CH}_3)_3$ ], 31.77 [s,  $\text{C}(\text{CH}_3)_3$ ], 32.80 (s,  $\text{CH}_2$ ), 34.08 [s,  $\text{C}(\text{CH}_3)_3$ ], 123.75 (s, aromatic CH), 129.28 (s, aromatic C), 143.81 (s, aromatic  $\text{C}t\text{Bu}$ ), 160.65 (s, aromatic CO); [ $\text{NC}(\text{CH}_3)_3$ ] not detectable. – IR (KBr) [**1a(NCMe)**]:  $\tilde{\nu} = 2959$   $\text{cm}^{-1}$  vs br ( $=\text{C}-\text{H}$ ), 2321 s ( $-\text{C}\equiv\text{N}$ ), 2292 m ( $-\text{C}\equiv\text{N}$ ), 1573 w, 1458 vs br, 1392 m, 1361 vs, 1304 s, 1282 s, 1243 vs br, 1197 vs br, 1125 m, 1105 s, 1025 w, 917 m, 870 s, 830 vs, 800 vs, 758 s, 677 m, 549 vs, 504 m, 424 s, 395 m. –  $^1\text{H}$  NMR ( $\text{CDCl}_3$ ) [**1a(CN $t$ Bu)**]:  $\delta = 7.04$  (s, 8 H, aromatic  $H$ ), 4.55 (d, 4 H,  $^2J_{\text{HH}} = 12.4$  Hz,  $\text{CH}_2$ ), 3.24 (d, 4 H,  $^2J_{\text{HH}} = 12.4$  Hz,  $\text{CH}_2$ ), 1.80 [s, 9 H,  $\text{NC}(\text{CH}_3)_3$ ], 1.20 [s, 36 H,  $\text{C}(\text{CH}_3)_3$ ],  $-0.20$  [s, 9 H,  $(\text{CH}_3)_3\text{CNC}$ ]. –  $^{13}\text{C}$  NMR ( $\text{CDCl}_3$ ) [**1a(CN $t$ Bu)**]:  $\delta = 28.62$  [s,  $\text{NC}(\text{CH}_3)_3$ ], 29.45 (s,  $\text{CH}_2$ ), 31.86 [s,  $\text{C}(\text{CH}_3)_3$ ], 33.96 [s,  $\text{C}(\text{CH}_3)_3$ ], 125.05 (s, aromatic CH), 127.90 (s, aromatic C), 143.69 (s, aromatic  $\text{C}t\text{Bu}$ ), 161.64 (s, aromatic CO); [ $\text{NC}(\text{CH}_3)_3$ ] not detectable. – IR (KBr) [**1a(CN $t$ Bu)**]:  $\tilde{\nu} = 2963$   $\text{cm}^{-1}$  vs br ( $=\text{C}-\text{H}$ ), 2211 m ( $-\text{C}\equiv\text{N}$ ), 1760 w, 1570 w, 1457 vs br, 1393 m, 1361 s, 1285 vs br, 1245 s, 1197 vs br, 1122 m, 1105 s, 1024 w, 959 w, 915 s, 872 s, 832 vs, 800 vs, 757 s, 709 w, 677 m, 631 m, 554 vs, 501 m, 422 vs, 390 m.

**Preparation of  $p\text{-tert-Butylcalix[4]arene-tert-butylimidotungsten(VI)}$  (**1b**):** A solution of 250 mg (0.53 mmol) of  $\text{W}(\text{NH}t\text{Bu})_2(\text{N}t\text{Bu})_2$  and 398 mg (0.53 mmol) of  $p\text{-}t\text{Bu-calix[4]arene}$  toluene adduct in 40 mL of toluene was stirred for 12 h at 60°C. All volatiles were removed in vacuo. The yellow residue was washed with 20 mL of hexane, collected, and dried in vacuo. Yield: 439 mg, 91%. m.p. 394°C (dec.). Crystals suitable for X-ray analysis were grown from saturated moist toluene solutions [**1b(OH<sub>2</sub>)**]. Yellow crystals of **1b(CN $t$ Bu)** could be obtained from solutions of **1b** in toluene and addition of an excess of  $t\text{Bu-isocyanide}$ . –  $^1\text{H}$  NMR ( $\text{CD}_2\text{Cl}_2$ ) [**1b**]:  $\delta = 7.12$  (s, 8 H, aromatic  $H$ ), 4.47 (d, 4 H,  $^2J_{\text{HH}} = 12.2$  Hz,  $\text{CH}_2$ ), 3.25 (d, 4 H,  $^2J_{\text{HH}} = 12.2$  Hz,  $\text{CH}_2$ ), 1.75 [s, 9 H,  $\text{NC}(\text{CH}_3)_3$ ], 1.20 [s, 36 H,  $\text{C}(\text{CH}_3)_3$ ]. –  $^{13}\text{C}$  NMR ( $\text{CD}_2\text{Cl}_2$ ) [**1b**]:  $\delta = 31.20$  [s,  $\text{NC}(\text{CH}_3)_3$ ], 31.87 [s,  $\text{C}(\text{CH}_3)_3$ ], 33.76 (s,  $\text{CH}_2$ ), 34.57 [s,  $\text{C}(\text{CH}_3)_3$ ], 75.81 [s,  $\text{NC}(\text{CH}_3)_3$ ], 125.21 (s, aromatic CH), 131.45 (s, aromatic C), 146.71 (s, aromatic  $\text{C}t\text{Bu}$ ), 152.29 (s, aromatic CO). – EI/MS (70 eV)  $m/z$  (%): 899 [ $\text{M}]^+$  (100), 884 [ $\text{M} - \text{CH}_3$ ] $^+$  (30), 842 [ $\text{M} - \text{C}_4\text{H}_9$ ] $^+$  (5), 828 [ $\text{M} - \text{NC}_4\text{H}_9$ ] $^+$  (42), 57 [ $\text{C}(\text{CH}_3)_3$ ] $^+$  (49). –



$C_{48}H_{61}NO_4W$  (899.87) calcd. C 64.07, H 6.83, N 1.56; found C 64.19, H 6.93, N 1.53.

$^1H$  NMR ( $CDCl_3$ ) [**1b**(OH<sub>2</sub>)]:  $\delta$  = 7.10 (s, 8 H, aromatic *H*), 4.58 (d, 4 H,  $^2J_{HH}$  = 12.4 Hz,  $CH_2$ ), 3.23 (d, 4 H,  $^2J_{HH}$  = 12.4 Hz,  $CH_2$ ), 1.75 [s, 9 H, NC( $CH_3$ )<sub>3</sub>], 1.54 (s, 2 H,  $H_2O$ ), 1.22 [s, 36 H, C( $CH_3$ )<sub>3</sub>]. –  $^{13}C$  NMR ( $CDCl_3$ ) [**1b**(OH<sub>2</sub>)]:  $\delta$  = 30.52 [s, NC( $CH_3$ )<sub>3</sub>], 31.55 [s, C( $CH_3$ )<sub>3</sub>], 32.94 (s,  $CH_2$ ), 33.98 [s, C( $CH_3$ )<sub>3</sub>], 71.59 [s, NC( $CH_3$ )<sub>3</sub>], 124.95 (s, aromatic CH), 130.57 (s, aromatic C), 144.52 (s, aromatic *CrBu*), 155.11 (s, aromatic CO). – IR (KBr) [**1b**(OH<sub>2</sub>)]:  $\tilde{\nu}$  = 3519  $cm^{-1}$  m (O–H), 3448 m (O–H), 2953 vs br (=C–H), 1751 w, 1570 m, 1471 vs br, 1394 s, 1361 vs, 1284 s br, 1199 vs, 1124 m, 1106 m, 1026 w, 917 m, 873 s, 834 vs, 800 s, 760 s, 678 m, 552 s, 503 m, 420 s.

$^1H$  NMR ( $CDCl_3$ ) [**1b**(NCMe)]:  $\delta$  = 7.05 (s, 8 H, aromatic *H*), 4.51 (d, 4 H,  $^2J_{HH}$  = 12.4 Hz,  $CH_2$ ), 3.18 (d, 4 H,  $^2J_{HH}$  = 12.4 Hz,  $CH_2$ ), 1.70 [s, 9 H, NC( $CH_3$ )<sub>3</sub>], 1.15 [s, 36 H, C( $CH_3$ )<sub>3</sub>], – 0.20 (s, 3 H, MeCN). –  $^{13}C$  NMR ( $CDCl_3$ ) [**1b**(NCMe)]:  $\delta$  = – 2.32 (s,  $CH_3$ CN), 30.38 [s, NC( $CH_3$ )<sub>3</sub>], 31.57 [s, C( $CH_3$ )<sub>3</sub>], 32.28 (s,  $CH_2$ ), 33.81 [s, C( $CH_3$ )<sub>3</sub>], 71.12 [s, NC( $CH_3$ )<sub>3</sub>], 123.46 (s, aromatic CH), 125.64 (s,  $CH_3$ CN), 130.31 (s, aromatic C), 143.57 (s, aromatic *CrBu*), 158.31 (s, aromatic CO). – IR (KBr) [**1b**(NCMe)]:  $\tilde{\nu}$  = 2953  $cm^{-1}$  vs br (=C–H), 2324 s (–C≡N), 2294 m (–C≡N), 1748 w, 1577 m, 1479 vs br, 1393 s, 1361 vs, 1272 vs br, 1196 vs, 1126 s, 1106 s, 1026 w, 917 m, 870 s, 833 vs, 800 s, 760 s, 678 m, 548 s, 504 m, 422 s. –  $^1H$  NMR ( $CDCl_3$ ) [**1b**(CN*rBu*)]:  $\delta$  = 7.13 (s, 8 H, aromatic *H*), 4.80 (d, 4 H,  $^2J_{HH}$  = 12.4 Hz,  $CH_2$ ), 3.35 (d, 4 H,  $^2J_{HH}$  = 12.4 Hz,  $CH_2$ ), 1.72 [s, 9 H, NC( $CH_3$ )<sub>3</sub>], 1.26 [s, 36 H, C( $CH_3$ )<sub>3</sub>], – 0.17 [s, 9 H, CNC( $CH_3$ )<sub>3</sub>]. –  $^{13}C$  NMR ( $CDCl_3$ ) [**1b**(CN*rBu*)]:  $\delta$  = 21.42 [s, (CH<sub>3</sub>)<sub>3</sub>CNC], 29.31 [s, NC( $CH_3$ )<sub>3</sub>], 31.72 [s, C( $CH_3$ )<sub>3</sub>], 33.62 (s,  $CH_2$ ), 33.91 [s, C( $CH_3$ )<sub>3</sub>], 70.67 [s, NC( $CH_3$ )<sub>3</sub>], 124.99 (s, aromatic CH), 129.21 (s, aromatic C), 143.61 (s, aromatic *CrBu*), 159.49 (s, aromatic CO). – IR (KBr) [**1b**(CN*rBu*)]:  $\tilde{\nu}$  = 2963  $cm^{-1}$  vs br (=C–H), 2218 m (–C≡N), 1758 w, 1604 m, 1573 m, 1477 vs br, 1393 m, 1361 s, 1285 vs br, 1197 vs br, 1124 s, 1105 s, 1029 w, 916 m, 874 s, 835 vs, 799 vs, 759 s, 731 vs, 695 s, 678 m, 552 vs, 502 m, 465 m, 419 s.

**Preparation of *p*-tert-Butylcalix[4]arenemesitylimidomolybdenum(VI) (2a):** A solution of 250 mg (0.48 mmol) of Mo(NMes)<sub>2</sub>Cl<sub>2</sub> · dme and 354 mg (0.48 mmol) of *p*-*t*Bu-calix[4]arene toluene adduct in 40 mL of toluene was stirred for 12 h at 100 °C. All volatiles were removed in vacuo and the yellow-brownish residue was extracted into 60 mL of hexane. Evaporation of the orange solution left a dark yellow solid, which was washed with 5 mL of pentane and dried in vacuo. Yield: 419 mg, 89%. m.p. 391 °C (dec.). Crystals in form of **2a**(NCMe), suitable for X-ray analysis, were grown from a saturated acetonitrile solution of **2a**. –  $^1H$  NMR ( $CDCl_3$ ) [**2a**]:  $\delta$  = 7.09 (s, 8 H, aromatic *H*), 6.93 (s, 2 H, Mes-*H<sub>m</sub>*), 4.41 (d, 4 H,  $^2J_{HH}$  = 12.4 Hz,  $CH_2$ ), 3.19 (d, 4 H,  $^2J_{HH}$  = 12.4 Hz,  $CH_2$ ), 3.07 [s, 6 H, Mes-( $CH_3$ )<sub>o</sub>], 2.44 [s, 3 H, Mes-( $CH_3$ )<sub>p</sub>], 1.21 [s, 36 H, C( $CH_3$ )<sub>3</sub>]. –  $^{13}C$  NMR ( $CDCl_3$ ) [**2a**]:  $\delta$  = 20.54 (Mes-*o*-CH<sub>3</sub>), 22.65 (s, Mes-*p*-CH<sub>3</sub>), 31.56 [s, C( $CH_3$ )<sub>3</sub>], 33.30 (s,  $CH_2$ ), 34.08 [s, C( $CH_3$ )<sub>3</sub>], 125.04 (s, aromatic CH), 125.93 (s, Mes-C-3), 129.41 (s, aromatic C), 140.13 (s, Mes-C-4), 141.97 (s, Mes-C-2), 144.69 (s, aromatic *CrBu*), 146.85 (s, Mes-C-1), 157.70 (s, aromatic CO). – EI/MS (70 eV) *m/z* (%): 875 [M]<sup>+</sup> (100), 860 [M – CH<sub>3</sub>]<sup>+</sup> (52), 428 [M – 2(CH<sub>3</sub>)]<sup>++</sup> (8). –  $^1H$  NMR ( $CDCl_3$ ) [**2a**(NCMe)]:  $\delta$  = 7.14 (s, 8 H, aromatic *H*), 6.97 (s, 2 H, Mes-*H<sub>m</sub>*), 4.47 (d, 4 H,  $^2J_{HH}$  = 12.4 Hz,  $CH_2$ ), 3.24 (d, 4 H,  $^2J_{HH}$  = 12.4 Hz,  $CH_2$ ), 3.12 [s, 6 H, Mes-( $CH_3$ )<sub>o</sub>], 2.49 [s, 3 H, Mes-( $CH_3$ )<sub>p</sub>], 1.27 [s, 36 H, C( $CH_3$ )<sub>3</sub>], – 0.11 (s, 3 H,  $CH_3$ CN). –  $^{13}C$  NMR ( $CDCl_3$ ) [**2a**(NCMe)]:  $\delta$  = – 2.13 (s,  $CH_3$ CN), 18.66 (Mes-*o*-CH<sub>3</sub>), 21.49 (s, Mes-*p*-CH<sub>3</sub>), 31.65 [s, C( $CH_3$ )<sub>3</sub>], 32.38 (s,  $CH_2$ ), 33.99 [s, C( $CH_3$ )<sub>3</sub>],

116.34 (s,  $CH_3$ CN), 123.67 (s, aromatic CH), 125.03 (s, Mes-C-3), 129.21 (s, aromatic C), 140.10 (s, Mes-C-4), 142.13 (s, Mes-C-2), 143.81 (s, aromatic *CrBu*), 144.68 (s, mes-C-1), 161.12 (s, aromatic CO). – IR (KBr) [**2a**(NCMe)]:  $\tilde{\nu}$  = 2950  $cm^{-1}$  st br (=C–H), 2323 m (–C≡N), 2293 m (–C≡N), 1739 w, 1600 m (C=C), 1455 vs br, 1362 m, 1300 m, 1197 vs, 1124 m, 1104 m, 915 m, 870 s, 829 vs, 799 vs, 757 st, 677 m, 548 vs, 505 m, 419 m. – C<sub>55</sub>H<sub>66</sub>MoN<sub>2</sub>O<sub>4</sub> (915.1) calcd. C 72.19, H 7.27, N 3.06; found C 71.61, H 6.94, N 3.25.

**Preparation of *p*-tert-Butylcalix[4]arenemesitylimidotungsten(VI) (2b):** A solution of 500 mg (0.82 mmol) of W(NMes)<sub>2</sub>Cl<sub>2</sub> · dme and 606 mg (0.82 mmol) of *p*-*t*Bu-calix[4]arene toluene adduct in 50 mL of toluene was stirred for 12 h at 100 °C. All volatiles were removed in vacuo and the red-orange residue was dissolved in 40 mL of hot acetone, filtered through a pad of celite and the solvent was removed in vacuo. The yellow residue was extracted into 60 mL of hexane. Evaporation of the solution gave a yellow powder, which was dried in vacuo. Yield: 677 mg, 86%. Crystals suitable for X-ray analysis were grown from saturated acetonitrile solutions of **2b** to give yellow crystals of **2b**(NCMe). –  $^1H$  NMR ( $CDCl_3$ ) [**2b**]:  $\delta$  = 7.12 (s, 8 H, aromatic *H*), 6.99 (s, 2 H, Mes-*H<sub>m</sub>*), 4.62 (d, 4 H,  $^2J_{HH}$  = 12.4 Hz,  $CH_2$ ), 3.25 (d, 4 H,  $^2J_{HH}$  = 12.4 Hz,  $CH_2$ ), 3.04 [s, 6 H, Mes-( $CH_3$ )<sub>o</sub>], 2.52 [s, 3 H, Mes-( $CH_3$ )<sub>p</sub>], 1.22 [s, 36 H, C( $CH_3$ )<sub>3</sub>]. –  $^{13}C$  NMR ( $CDCl_3$ ) [**2b**]:  $\delta$  = 18.10 (Mes-*o*-CH<sub>3</sub>), 20.96 (s, Mes-*p*-CH<sub>3</sub>), 31.58 [s, C( $CH_3$ )<sub>3</sub>], 33.09 (s,  $CH_2$ ), 34.06 [s, C( $CH_3$ )<sub>3</sub>], 125.08 (s, aromatic CH), 127.28 (s, Mes-C-3), 130.58 (s, aromatic C), 137.79 (s, Mes-C-4), 140.05 (s, Mes-C-2), 144.85 (s, aromatic *CrBu*), 145.65 (s, Mes-C-1), 155.35 (s, aromatic CO). – EI/MS (70 eV) *m/z* (%): 961 [M]<sup>+</sup> (100), 946 [M – CH<sub>3</sub>]<sup>+</sup> (46), 930 [M – 2CH<sub>3</sub>]<sup>+</sup> (2), 466 [M – 2CH<sub>3</sub>]<sup>++</sup> (46). – C<sub>53</sub>H<sub>63</sub>NO<sub>4</sub>W (961.94) calcd. C 66.18, H 6.60, N 1.46; found C 65.88, H 6.69, N 1.53.

$^1H$  NMR ( $CDCl_3$ ) [**2b**(NCMe)]:  $\delta$  = 7.14 (s, 8 H, aromatic *H*), 6.98 (s, 2 H, Mes-*H<sub>m</sub>*), 4.59 (d, 4 H,  $^2J_{HH}$  = 12.4 Hz,  $CH_2$ ), 3.25 (d, 4 H,  $^2J_{HH}$  = 12.4 Hz,  $CH_2$ ), 3.02 [s, 6 H, Mes-( $CH_3$ )<sub>o</sub>], 2.51 [s, 3 H, Mes-( $CH_3$ )<sub>p</sub>], 1.18 [s, 36 H, C( $CH_3$ )<sub>3</sub>], – 0.12 (s, 3 H,  $CH_3$ CN). –  $^{13}C$  NMR ( $CDCl_3$ ) [**2b**(NCMe)]:  $\delta$  = – 2.00 (s,  $CH_3$ CN), 18.09 (Mes-*o*-CH<sub>3</sub>), 20.93 (s, Mes-*p*-CH<sub>3</sub>), 31.67 [s, C( $CH_3$ )<sub>3</sub>], 32.51 (s,  $CH_2$ ), 33.92 [s, C( $CH_3$ )<sub>3</sub>], 116.27 (s,  $CH_3$ CN), 123.63 (s, aromatic CH), 127.19 (s, Mes-C-3), 130.42 (s, aromatic C), 137.47 (s, Mes-C-4), 140.33 (s, Mes-C-2), 143.93 (s, aromatic *CrBu*), 149.49 (s, Mes-C-1), 158.74 (s, aromatic CO). – IR (KBr) [**2b**(NCMe)]:  $\tilde{\nu}$  = 2953  $cm^{-1}$  st br (=C–H), 2323 m (–C≡N), 2294 m (–C≡N), 1734 w, 1605 m (C=C), 1478 vs br, 1393 m, 1361 m, 1304 m, 1274 s, 1244 s, 1195 vs, 1126 m, 1105 m, 1021 w br, 945 w, 920 m, 871 s, 833 vs, 800 vs, 761 st, 727 m, 678 m, 589 m, 549 s, 504 m, 421 m.

**Crystal Structure Analysis of 1a(NCMe):** Stoe-STADI IV diffractometer (Mo-*K $\alpha$*  radiation), *T* = 200(2) K; data collection and refinement: SHELXS-97<sup>[25]</sup> and SHELXL-97<sup>[26]</sup> orthorhombic, space group Cmc2<sub>1</sub>; lattice constants *a* = 14.338(3), *b* = 21.066(4), *c* = 19.586(4) Å, *V* = 5916(2) Å<sup>3</sup>, *Z* = 4,  $\mu$ (Mo-*K $\alpha$* ) = 0.259 mm<sup>–1</sup>, 2 $\theta_{max}$  = 51.9°; 3104 independent reflections measured, of which 2829 were considered observed with *I* > 2 $\sigma$ (*I*); max./min. residual electronic density 1.141 and –0.638 e/Å<sup>3</sup>; 259 parameters (W, O, N, anisotropic, C anisotropic except disordered *t*Bu groups, the positions of the H atoms were calculated for idealized positions); *R*<sub>1</sub> = 0.070; *wR*<sub>2</sub> = 0.1923.

**Crystal Structure Analysis of 1b(OH<sub>2</sub>):** Stoe-STADI IV diffractometer (Mo-*K $\alpha$*  radiation), *T* = 200(2) K; data collection and refinement: SHELXS-97<sup>[25]</sup> and SHELXL-97<sup>[26]</sup> orthorhombic, space group Cmc2<sub>1</sub>; lattice constants *a* = 15.013(3), *b* = 20.633(4), *c* = 19.448(4) Å, *V* = 6024(2) Å<sup>3</sup>, *Z* = 4,  $\mu$ (Mo-*K $\alpha$* ) = 1.956 mm<sup>–1</sup>,

$2\Theta_{\max} = 55.0^\circ$ ; 6222 independent reflections measured, of which 6024 were considered observed with  $I > 2\sigma(I)$ ; max./min. residual electronic density 0.772 and  $-0.628 \text{ e}/\text{\AA}^3$ ; 250 parameters (W, O, N, anisotropic, C anisotropic except disordered *t*Bu groups, the positions of the H atoms were calculated for idealized positions);  $R_1 = 0.031$ ;  $wR_2 = 0.0908$ .

**Crystal Structure Analysis of 1b(CN*t*Bu):** Stoe-STADI IV diffractometer (Mo-*K* $\alpha$  radiation),  $T = 203(2) \text{ K}$ ; data collection and refinement: SHELXS-97<sup>[25]</sup> and SHELXL-97;<sup>[26]</sup> orthorhombic, space group Cmc<sub>21</sub>; lattice constants  $a = 15.503(3)$ ,  $b = 20.480(4)$ ,  $c = 19.617(4) \text{ \AA}$ ,  $V = 6228(2) \text{ \AA}^3$ ,  $Z = 4$ ,  $\mu(\text{Mo-}K_{\alpha}) = 1.889 \text{ mm}^{-1}$ ,  $2\Theta_{\max} = 50.3^\circ$ ; 2981 independent reflections measured, of which 2896 were considered observed with  $I > 2\sigma(I)$ ; max./min. residual electronic density 1.229 and  $-0.584 \text{ e}/\text{\AA}^3$ ; 268 parameters (W, O, N, anisotropic, C anisotropic except disordered *t*Bu groups, the positions of the H atoms were calculated for idealized positions);  $R_1 = 0.043$ ;  $wR_2 = 0.1420$ .

**Crystal Structure Analysis of 2a(NCMe):** Stoe-IPDS diffractometer (Mo-*K* $\alpha$  radiation),  $T = 200(2) \text{ K}$ ; data collection and refinement: SHELXS-97<sup>[25]</sup> and SHELXL-97;<sup>[26]</sup> triclinic, space group  $P\bar{1}$ ; lattice constants  $a = 11.015(6)$ ,  $b = 11.970(9)$ ,  $c = 18.574(11) \text{ \AA}$ ,  $\alpha = 93.06(7)$ ,  $\beta = 93.52(6)$ ,  $\gamma = 96.53(7)^\circ$ ,  $V = 2424(3) \text{ \AA}^3$ ,  $Z = 2$ ,  $\mu(\text{Mo-}K_{\alpha}) = 0.317 \text{ mm}^{-1}$ ,  $2\Theta_{\max} = 54.3^\circ$ ; 9809 independent reflections measured, of which 8510 were considered observed with  $I > 2\sigma(I)$ ; max./min. residual electronic density 0.805 and  $-1.116 \text{ e}/\text{\AA}^3$ ; 574 parameters (W, O, N, anisotropic, C anisotropic except disordered *t*Bu groups, the positions of the H atoms were calculated for idealized positions);  $R_1 = 0.052$ ;  $wR_2 = 0.1427$ .

**Crystal Structure Analysis of 2b(NCMe):** Stoe-STADI IV diffractometer (Mo-*K* $\alpha$  radiation),  $T = 203(2) \text{ K}$ ; data collection and refinement: SHELXS-97<sup>[25]</sup> and SHELXL-97;<sup>[26]</sup> triclinic, space group Cc; lattice constants  $a = 13.122(3)$ ,  $b = 19.416(4)$ ,  $c = 20.535(4) \text{ \AA}$ ,  $\beta = 99.86(3)^\circ$ ,  $V = 5154.6(18) \text{ \AA}^3$ ,  $Z = 4$ ,  $\mu(\text{Mo-}K_{\alpha}) = 2.288 \text{ mm}^{-1}$ ,  $2\Theta_{\max} = 54.0^\circ$ ; 6638 independent reflections measured, of which 6217 were considered observed with  $I > 2\sigma(I)$ ; max./min. residual electronic density 0.461 and  $-0.605 \text{ e}/\text{\AA}^3$ ; 588 parameters (W, O, N, C anisotropic except solvent molecules, the positions of the H atoms were calculated for idealized positions);  $R_1 = 0.019$ ;  $wR_2 = 0.049$ .

Crystallographic data (excluding structure factors) for the structures reported in this paper have been deposited with the Cambridge Crystallographic Data Centre as supplementary publication nos. CCDC-114936 to CCDC-114940. Copies of the data can be obtained free of charge on application to CCDC, 12 Union Road, Cambridge, CB2 1EZ, UK (Fax: +44 1223/336 033; E-mail: deposit@ccdc.cam.ac.uk).

## Acknowledgments

This work was supported by the Deutsche Forschungsgemeinschaft and the Fonds der Chemischen Industrie (Liebig fellowship for U. R.). U. R. kindly thanks Professor D. Fenske for his continued support and interest in our work. Furthermore, we would like to thank Dr. S. Elliott for helpful discussions as well as Dr. E. Matern and H. Berberich for recording NMR spectra. A gift of metal chlorides from Fa. H. C. Starck GmbH, Goslar, is gratefully acknowledged.

[1] [1a] W. A. Nugent, B. L. Haymore, *Coord. Chem. Rev.* **1980**, *31*, 123–175. – [1b] W. A. Nugent, J. M. Mayer, *Metal-Ligand Multiple Bonds*, Wiley, New York, **1988**. – [1c] D. E. Wigley, *Prog. Inorg. Chem.* **1994**, *42*, 239–482.

- [2] [2a] R. R. Schrock: *Olefin Metathesis by Well-Defined Complexes of Molybdenum and Tungsten* in: A. Fürstner (Ed.), *Topics in Organometallic Chemistry, Vol. 1: Metathesis in Organic Synthesis*, Springer-Verlag, Berlin **1999**, 1–36. – [2b] C. J. Schaverian, J. C. Dewan, R. R. Schrock, *J. Am. Chem. Soc.* **1986**, *108*, 2771–2773. – [2c] J. S. Murdzek, R. R. Schrock, *Organometallics* **1987**, *6*, 1373–1374. – [2d] R. R. Schrock, R. T. DePue, J. Feldman, K. B. Yap, W. M. Davies, L. Park, M. DiMare, M. Schofield, J. Anhaus, E. Walborski, E. Evitt, C. Krüger, P. Betz, *Organometallics* **1990**, *9*, 2262–2275. – [2e] M. A. Andrews, H. D. Kaesz, *J. Am. Chem. Soc.* **1977**, *99*, 6763–6765.
- [3] [3a] G. W. Parshall, W. A. Nugent, D. M.-T. Chan, W. Tam, *Pure Appl. Chem.* **1985**, *12*, 1809–1818. – [3b] E. Herranz, S. A. Biller, K. B. Sharpless, *J. Am. Chem. Soc.* **1978**, *100*, 3596–3598. – [3c] W. D. Patrick, L. K. Truesdale, S. A. Biller, K. B. Sharpless, *J. Org. Chem.* **1978**, *13*, 2628–2638. – [3d] R. Breslow, R. Q. Kluttz, P. L. Khanna, *Tetrahedron Lett.* **1979**, *35*, 3273–3274. – [3e] T.-L. Ho, M. Henninger, G. A. Olah, *Synthesis* **1976**, 815–816.
- [4] R. K. Grasselli, *J. Chem. Ed.* **1986**, *63*, 216–221.
- [5] [5a] J. D. Bunting, R. K. Grasselli, *J. Catal.* **1979**, *59*, 79–99. – [5b] J. D. Bunting, C. T. Kartisek, R. K. Grasselli, *J. Catal.* **1981**, *69*, 495–497. – [5c] J. D. Bunting, C. T. Kartisek, R. K. Grasselli, *J. Catal.* **1984**, *87*, 363–380. – [5d] D. M.-T. Chan, W. A. Nugent, *Inorg. Chem.* **1985**, *24*, 1422–1424. – [5e] D. M.-T. Chan, W. C. Fultz, W. A. Nugent, D. C. Roe, T. H. Tulip, *J. Am. Chem. Soc.* **1985**, *107*, 251–253. – [5f] G. W. Keulks, L. D. Krenzke, T. M. Notermann, *Adv. Catal.* **1978**, *27*, 183–225. – [5g] K. Brueckmann, J. Haber, T. Wiltkowski, *J. Catal.* **1987**, *106*, 188–193. – [5h] E. A. Maata, Y. Du, *J. Am. Chem. Soc.* **1988**, *110*, 8249–8250. – [5i] E. A. Maata, Y. Du, A. L. Rheingold, *J. Chem. Soc., Chem. Commun.* **1990**, 756–757. – [5j] J. Belgacem, J. Kress, J. A. Osborn, *J. Chem. Soc., Chem. Commun.* **1993**, 1125–1127.
- [6] [6a] C. D. Gutsche, *Calixarenes*, The Royal Society of Chemistry, Cambridge **1989**. – [6b] J. Vincens, V. Böhmer (Eds.), *Calixarenes: A Versatile Class of Macrocyclic Compounds*, Kluwer, Dordrecht **1991**. – [6c] C. D. Gutsche, *Prog. Macrocycl. Chem.* **1987**, *3*, 93–165. – [6d] V. Böhmer, *Angew. Chem.* **1995**, *107*, 785–818; *Angew. Chem. Int. Ed. Engl.* **1995**, *34*, 713–745.
- [7] [7a] D. M. Roundhill, *Prog. Inorg. Chem.* **1995**, *43*, 533–565. – [7b] C. Wieser, C. B. Dieleemann, D. Matt, *Coord. Chem. Rev.* **1997**, *165*, 93–61. – [7c] C. Floriani, *Chem. Eur. J.* **1999**, *5*, 19–23. – For tungsten calixarene carbene and carbyne complexes related to the imido complexes presented here see: [7d] L. Giannini, E. Solari, S. Dovesi, C. Floriani, N. Re, A. Chiesi-Villa, C. Rizzoli, *J. Am. Chem. Soc.* **1999**, *121*, 2784–2796. – [7e] L. Giannini, G. Guillemont, E. Solari, C. Floriani, N. Re, A. Chiesi-Villa, C. Rizzoli, *J. Am. Chem. Soc.* **1999**, *121*, 2797–2807 and references cited therein.
- [8] U. Radius, J. Attner, *Eur. J. Inorg. Chem.* **1998**, 299–303.
- [9] [9a] V. C. Gibson, C. Redshaw, W. Clegg, M. R. J. Elsegood, *J. Chem. Soc., Chem. Commun.* **1995**, 2371–2381. – [9b] V. C. Gibson, C. Redshaw, W. Clegg, M. R. J. Elsegood, *J. Chem. Soc., Chem. Commun.* **1997**, 1605–1606.
- [10] [10a] P. W. Dyer, V. C. Gibson, J. A. K. Howard, B. Whittle, C. Wilson, *J. Chem. Soc., Chem. Commun.* **1992**, 1666–1668. – [10b] A. A. Danopoulos, G. Wilkinson, B. Hussain-Bates, M. B. Hursthouse, *J. Chem. Soc., Dalton Trans.* **1990**, 2753–2761. – [10c] W. A. Nugent, *Inorg. Chem.* **1983**, *22*, 965–969. – [10d] W. A. Nugent, R. L. Harlow, *Inorg. Chem.* **1990**, *19*, 777–779.
- [11] Reaction of **1a** and **1b** with reagents like pyridinium(HCl) lead reversibly to adducts of the general formula LM(Cl)(NH*t*Bu). Reaction of **1b** with a small excess of HCl (> 2 equiv.) yields LWCl<sub>2</sub>, and with a larger amount of HCl to decomposition of the compound: U. Radius, J. Attner, unpublished results.
- [12] U. Radius, J. Sundermeyer, H. Pritzkow, *Chem. Ber.* **1994**, *127*, 1827–1835.
- [13] F. Corazza, C. Floriani, A. Chiesi-Villa, C. Guastini, *J. Chem. Soc., Chem. Commun.* **1990**, 640–641.
- [14] [14a] F. Hajek, E. Graf, M. W. Hosseini, X. Delaigue, A. De Cian, J. Fischer, *Tetrahedron Lett.* **1996**, *37*, 1401–1404. – [14b] F. Hajek, M. W. Hosseini, E. Graf, A. De Cian, J. Fischer, *Angew. Chem.* **1997**, *109*, 1830–1832; *Angew. Chem., Int. Ed. Engl.* **1997**, *36*, 1760–1762. – [14c] A. Zanotti-Gerosa, E. Solari, L. Giannini, C. Floriani, A. Chiesi-Villa, C. Rizzoli, *J. Chem. Soc., Chem. Commun.* **1996**, 119–120. – [14d] B. Xu, T. M. Swager, *J. Am. Chem. Soc.* **1993**, *115*, 1159–1160.

- [15] G. D. Andreotti, R. Ungaro, A. Pochini, *J. Chem. Soc., Chem. Commun.* **1979**, 1005–1007.
- [16] [16a] H. W. Roesky, J. Sundermeyer, J. Schimkowiak, P. G. Jones, M. Noltemeyer, T. Schroeder, G. M. Sheldrick, *Z. Naturforsch.* **1985**, *40B*, 736–739. – [16b] M. Witt, H. W. Roesky, M. Noltemeyer, G. M. Sheldrick, *Z. Naturforsch.* **1987**, *42B*, 519–521. – [16c] A. Görges, K. Dehnicke, D. Fenske, *Z. Naturforsch.* **1988**, *43B*, 677–681.
- [17] D. J. Szalda, J. C. Dewan, S. J. Lippard, *Inorg. Chem.* **1981**, *20*, 3851–3857.
- [18] [18a] J. L. Atwood, S. G. Bott, P. C. Junk, M. T. May, *J. Coord. Chem.* **1996**, *37*, 89–105. – [18b] Y. Jeannin, J.-P. Launay, J. Livage, A. Nel, *Inorg. Chem.* **1978**, *17*, 374–378.
- [19] G. Orpen, *J. Chem. Soc., Dalton Trans.* **1989**, S1–S89.
- [20] C. Y. Chou, J. C. Huffman, E. A. Maata, *J. Chem. Soc., Chem. Commun.* **1984**, 1184–1185.
- [21] Density functional calculations were performed using the TURBOMOLE set of programs and applying the B-P86/SVP density functional within the RI-J approximation: [21a] R. Ahlrichs, *TURBOMOLE*, in: P. v. R. Schleyer (Ed.), *Encyclopedia of Computational Chemistry*, Wiley, Chichester **1998**, Vol. 5, 3123–3129. – [21b] R. Ahlrichs, M. v. Arnim, *TURBOMOLE, parallel implementation of SCF, density functional, and chemical shift modules*, in: E. Clementi, G. Corongiu (Eds.): *Methods and Techniques in Computational Chemistry*, STEF, Cagliari **1995**; – [21c] K. Eichkorn, O. Treutler, H. Öhm, M. Häser, R. Ahlrichs, *Chem. Phys. Lett.* **1995**, *242*, 652–660. – For definition of the B-P86 density functional see: [21d] A. D. Becke, *Phys. Rev. A* **1988**, *38*, 3098–3100. – [21e] J. P. Perdew, *Phys. Rev. B* **1986**, *33*, 8822–8824; *erratum*: J. P. Perdew, *Phys. Rev. B* **1986**, *34*, 7406. – The acronym SVP refers to TURBOMOLE split valence basis sets, augmented by a shell of polarization functions, cf. [21f] A. Schäfer, H. Horn, R. Ahlrichs, *J. Chem. Phys.* **1992**, *97*, 2571–2577. – Quasi-relativistic pseudo potentials were used for the element W: [21g] D. Andrae, U. Häussermann, M. Dolg, H. Stoll, H. Preuss, *Theor. Chim. Acta* **1990**, *77*, 123–141.
- [22] The shared electron number SEN is based on population analysis and can serve as a measure of covalent bond strength: R. Ahlrichs, C. Erhardt, *Chem. Unserer Zeit* **1985**, *19*, 120–124. Some typical values for SEN provided in this paper: C–C, C–H: 1.4; C=C: 2.2; C≡C, N≡N: 3.3. Reduced SENs are found for polar bonds, like in NaF (0.3), and for weak bonds as in Cl<sub>2</sub> (0.9) and F<sub>2</sub> (0.6). For the calix[4]arene fragments of our compounds we calculate for aromatic carbon-carbon bonds (C=C)<sub>ar</sub> SENs of approximately 1.8, for C–C bonds to the methylene bridges SENs of approximately 1.4, and approximately 1.3 for C–H bonds.
- [23] J. A. Acho, L. H. Doerrer, S. J. Lippard, *Inorg. Chem.* **1995**, *34*, 2542–2776.
- [24] [24a] C. D. Gutsche, M. Iqbal, A. T. Watson, C. H. Heathcock, *Org. Synth.* **1989**, *68*, 234–237. – [24b] A. Arduini, A. Casnati, *Macrocyclic Synthesis, A Practical Approach*, Oxford University Press, New York, **1996**.
- [25] G. M. Sheldrick, *SHELXS-97. Program for Crystal Structure Solution*, Universität Göttingen, **1997**.
- [26] G. M. Sheldrick, *SHELXL-97. Program for Crystal Structure Refinement*, Universität Göttingen, **1997**.

Received February 22, 1999  
[199062]